

Power Allocation Algorithms for Massive MIMO Systems with Multi-Antenna Users

Evgeny Bobrov^{a,b}, Boris Chinyaev^a, Viktor Kuznetsov^b,
Dmitrii Minenkov^{a,c}, Daniil Yudakov^a

^a M.V. Lomonosov Moscow State University, Russia;

^b Huawei Technologies, Russian Research Institute, Moscow Research Center, Russia,

^c A. Ishlinsky Institute for Problems in Mechanics RAS, Russia

ARTICLE HISTORY

Compiled April 4, 2022

ABSTRACT

Modern 5G wireless cellular networks use massive multiple-input multiple-output (MIMO) technology. This concept entails using an antenna array at a base station to concurrently service many mobile devices that have several antennas on their side. In this field, a significant role is played by the precoding (beamforming) problem. During downlink, an important part of precoding is the power allocation problem that distributes power between transmitted symbols. In this paper, we consider the power allocation problem for a class of precodings that asymptotically work as regularized zero-forcing. Under some realistic assumptions, we simplify the sum spectral efficiency functional and obtain tractable expressions for it. We prove that equal power allocation provides optimum for the simplified functional with total power constraint (TPC). Also, low-complexity algorithms that improve equal power allocation in the case of per-antenna power constraints are proposed. On simulations using Quadriga, the proposed algorithms show a significant gain in sum spectral efficiency while using a similar computing time as the reference solutions.

KEYWORDS

5G, MIMO, Multi-antenna UE, Precoding, Regularized Zero-Forcing, Power Allocation, MMSE-IRC Detection, Constrained Optimization, Karush–Kuhn–Tucker conditions, Asymptotics

1. Introduction

The massive multiple-input multiple-output (MIMO) systems have attracted a lot of attention in both academia and industry since their first appearance [2, 24]. The main characteristic of the massive MIMO system is the large-scale antenna arrays at the cellular base station (BS). Using a large number of antennas, the massive MIMO system can exceed the achievable speed of a conventional MIMO [15] system and simultaneously serves (with low power consumption) several users.

A critical issue for improving the performance of wireless networks is the efficient management of available radio resources [21]. Numerous works are dedicated to optimal allocation of the radio resources, for example, power and bandwidth to improve the performance of wireless networks [29]. An important part of signal processing in

downlink is precoding since with this procedure we can focus transmission signal energy on smaller regions, which allows achieving greater spectral efficiency with lower transmitted power [2, 26]. Various linear precodings allow to direct the maximum amount of energy to the user like Maximum Ratio Transmission (MRT) or completely get rid of inter-user interference like Zero-Forcing (ZF) [28, 43]. The precoding problem is well-studied (see e.g. overview [13, 14, 45] and textbooks [2, 4, 34] and bibliography within), nonetheless there are open questions.

An important component of the precoding procedure is the power allocation (PA) problem that is widely discussed in the literature. In [12], by using either the signal-to-noise ratio (SNR) or the outage probability as the performance criteria, different power allocation (PA) strategies are developed to exploit the knowledge of channel means. In [17] bounds on the channel capacity are derived for a similar model with Rayleigh fading and channel state information (CSI). The bandwidth allocation problem in a three-node Gaussian orthogonal relay system is investigated in [22] to maximize a lower bound on the capacity. Two power allocation schemes based on minimization of the outage probability are presented in [44] for the case when the information of the wireless channel responses or statistics is available at the transmitter. In [27] studies optimal power allocation schemes in a multi-relay cooperating network employing amplify-and-forward protocol with multiple source-destination pairs. The work [31] advocates the use of deep learning to perform max-min and max-prod power allocation in the downlink of Massive MIMO networks. In [35] the total downlink power consumption at the access points is minimized, considering both the transmit powers and hardware dissipation.

The most relevant works to the current paper are of E. Björnson et. al. In [4, sec. 7.1] the case of one antenna user equipment (UE) is studied in detail, targeting UE spectral efficiency and using multi-criteria optimization approach and Pareto front analysis. In [5, p. 328] multi-antenna UEs are considered, but they are supposed to get only one data channel (or stream). The difficulty of the multi-antenna UE case is that the channels between different antennas of one UE are often spatial correlated [6]. Therefore, the matrix of the user channel is ill-conditioned (or even has incomplete rank) thus one can not efficiently transmit data using the maximum number of streams. To solve this problem, instead of the full matrix of the user channel, vectors from its singular value decomposition (SVD) with the largest singular values are used for precoding [33]. When the number of streams (UE rank) is greater than one then the phenomena of effective SINR are to be taken into account [16].

In this paper, we study the problem of power allocation (PA) of MIMO wireless systems with users with multiple antennas and generalize the results of E. Björnson et. al. for the case of multi-antenna UEs with rank greater than one. We present the novel solutions to the PA problem that maximize network throughput in terms of spectral efficiency (SE). Since the original problem is not convex, it is simplified to convex by selecting specific and widely used parameters of the MIMO system [2]. Usually, the total power constraint (TPC) (see e.g. [11]) or more realistic per-antenna power constraint (PAPC) are considered (see e.g. [5, 41]). Under some natural assumptions, we simplify the sum spectral efficiency functional and prove that the uniform power allocation provides its optimum subject to TPC. For the case of PAPC, we equivalently reformulate the optimization problem as the Lagrange system of equations and write down the Karush–Kuhn–Tucker conditions. Here algorithmic solutions of PA for PAPC are proposed. The simulation results show the effectiveness of the proposed algorithmic approach in comparison with the reference PA schemes. To the authors' best knowledge, these mathematical results are new.

Table 1. Symbols and notations

Symbols	Notations
$(\cdot)^H$	Complex conjugate operator
\mathbf{H}, \mathbf{W}	Matrices
\mathbf{w}_n	n -th column of matrix \mathbf{W}
$\mathbf{h}_k, \mathbf{w}^k$	k -th row of matrices \mathbf{H}, \mathbf{W}
h_{nm}, w_{nm}	n, m -th element of matrices \mathbf{H}, \mathbf{W}
$\mathbf{S} = \text{diag}(s_1, \dots, s_N)$	diagonal matrix
K	the number of users
T	the number of transmit antennas
R	the total number of receive antennas
R_k	the number of receive antennas for each user
L	the total number of layers in the system
L_k	the number of layers for each user

The rest of this paper is organized as follows. After this Introduction, Section 2 is devoted to the channel and system model where we introduce the downlink MIMO channel model, reference precoding methods, various detection schemes, and quality measures. In Section 3 we show a simplification of the PA problem, where we describe asymptotic diagonalization property of precoding matrices are used, proof of similarity of Conjugate and MMSE-IRC matrices, and Effective SINR models. In Section 4 we consider the problem of the PA algorithm under TPC and PAPC assumptions, where we describe equal power allocation under the TPC, and the solution under the PAPC assumptions, we also consider problem-solving taking into account QAM modulation (4.2) and numerical algorithm description (4.5). Numerical experiments to compare considered algorithms are provided in Section 5, and Section 6 contains a conclusion. Symbols and notations are shown in Tab. 1.

2. Channel and System Model

According to [1, 4, 34, 42] we consider a MIMO broadcast channel. Symbol $\mathbf{r} \in \mathbb{C}^L$ is a *received vector*, and $\mathbf{x} \in \mathbb{C}^L$ is a *sent vector*, and $\mathbf{H} \in \mathbb{C}^{R \times T}$ is a *channel matrix*, and $\mathbf{W} \in \mathbb{C}^{T \times L}$ is a *Precoding matrix*, and $\mathbf{G} \in \mathbb{C}^{L \times R}$ is a block-diagonal *detection matrix*, and $\mathbf{n} \sim \mathcal{CN}(0, I_L)$ is a *noise-vector*. Note that the linear precoding and detection are implemented by simple matrix multiplications. The constant T is the number of transmit antennas, R is the total number of receive antennas, and L is the total number of transmitted symbols in the system. Usually, they are related as $L \leq R \leq T$. Each of the matrices $\mathbf{G}, \mathbf{H}, \mathbf{W}$ decomposes by K *users*, so please see the scheme in Fig. 1. The Multi-User MIMO model is described using the following linear system:

$$\mathbf{r} = \mathbf{G}(\mathbf{H}\mathbf{W}\mathbf{x} + \mathbf{n}). \quad (1)$$

Throughout the paper, we assume that i) the channels of all users are subject to uncorrelated Rayleigh fading and, for simplicity, all users are homogeneous and experience

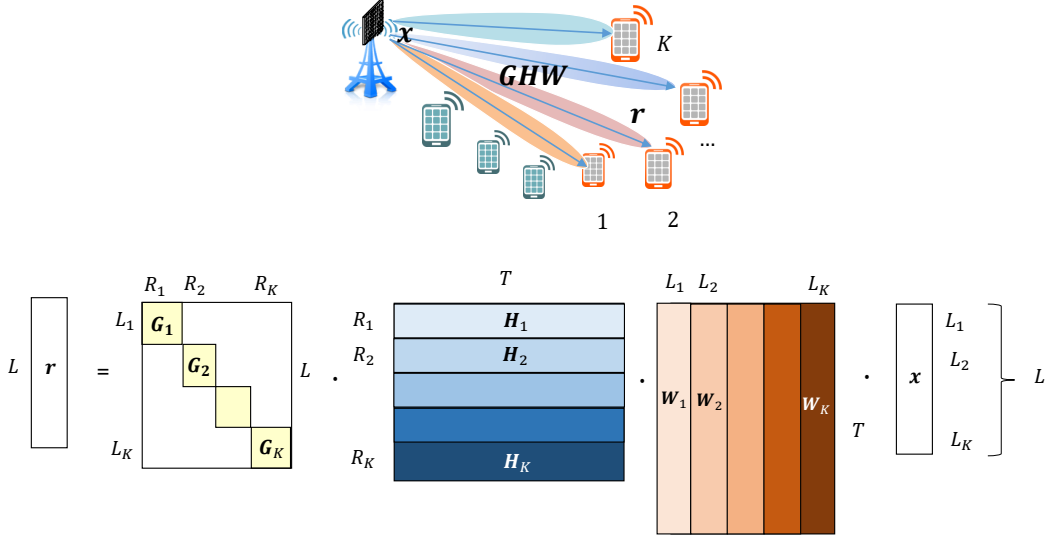


Figure 1. System model. Multi-User precoding allows to transmit different information to different users simultaneously. The problem is to find an optimal precoding matrix W of the system given the target Spectral Efficiency function [7].

statistically independent fading, ii) the transmitter has perfect CSI of all downlink channels, this assumption is reasonable in time division duplex (TDD) systems, which allows the transmitter to employ reciprocity to estimate the downlink channels, and iii) each user only has access to their own CSI, but not the CSI of the downlink channels of the other users.

2.1. Singular Value Decomposition of the Channel

The *channel matrix* for user k , $\mathbf{H}_k \in \mathbb{C}^{R_k \times T}$ contains channel vectors $\mathbf{h}_i \in \mathbb{C}^T$ by rows. The *path loss* diagonal matrix $\mathbf{S}_k \in \mathbb{R}^{R_k \times R_k}$ contains R_k singular values σ_{kn} in decreasing order along its main diagonal. It is convenient [33] to represent \mathbf{H}_k via its Singular Value Decomposition (SVD):

$$\mathbf{H}_k = \mathbf{U}_k^H \mathbf{S}_k \mathbf{V}_k, \quad (2)$$

Lemma 2.1 (Main Decomposition). [7] Denote $\mathbf{H} = [\mathbf{H}_1, \dots, \mathbf{H}_K] \in \mathbb{C}^{R \times T}$ the concatenation of individual channel rows \mathbf{H}_k . Similarly, $\mathbf{U} = \text{bdiag}\{\mathbf{U}_1, \dots, \mathbf{U}_K\}$, $\mathbf{S} = \text{diag}\{\mathbf{S}_1, \dots, \mathbf{S}_K\}$, $\mathbf{V} = [\mathbf{V}_1, \dots, \mathbf{V}_K]$. The following representation holds

$$\mathbf{H} = \mathbf{U}^H \mathbf{S} \mathbf{V}. \quad (3)$$

where the $\mathbf{H} \in \mathbb{C}^{R \times T}$, and $\mathbf{S} = \text{diag}(\mathbf{S}_k) \in \mathbb{C}^{R \times R}$, and $\mathbf{U} = \text{bdiag}(\mathbf{U}_k) \in \mathbb{C}^{R \times R}$ is block-diagonal unitary matrix, $\mathbf{V} = [\mathbf{V}_1, \dots, \mathbf{V}_K] \in \mathbb{C}^{R \times T}$ is the concatenation of corresponding UE singular vectors because $\mathbf{C} = \mathbf{V} \mathbf{V}^H - \mathbf{I} \neq \mathbf{O}$.

Lemma 2.1 means that by collecting all users together we can write a specific *channel matrix* decomposition [7]. Note, that such decomposition is not a convenient SVD of the channel matrix \mathbf{H} , and matrix \mathbf{V} is not unitary. But it consists of the K SVD-

decompositions of the size $R_k \times T$ and has block-diagonal unitary left matrix \mathbf{U} . We use this form in the construction of the optimal *detection matrix* \mathbf{G} [33].

Usually, the transmitter sends to UE several layers and the number of layers (rank) is less than the number of UE antennas ($L_k \leq R_k$). In this case, it is natural to choose for transmission the first L_k vectors from $\tilde{\mathbf{V}}_k$ that correspond to the L_k largest singular values from $\tilde{\mathbf{S}}_k$. Denote by $\tilde{\mathbf{S}}_k \in \mathbb{C}^{L_k \times L_k}$ the first L_k largest singular values from \mathbf{S}_k , and by $\tilde{\mathbf{U}}_k^H \in \mathbb{C}^{R_k \times L_k}$, $\tilde{\mathbf{V}}_k \in \mathbb{C}^{L_k \times T}$ the first L_k left and right singular vectors that correspond to $\tilde{\mathbf{S}}_k$:

$$\tilde{\mathbf{S}}_k = \text{diag}\{s_{k,1}, \dots, s_{k,L_k}\}, \quad \tilde{\mathbf{U}}_k^H = (\mathbf{u}_{k,1}^H, \dots, \mathbf{u}_{k,L_k}^H), \quad \tilde{\mathbf{V}}_k = [\mathbf{v}_{k,1}; \dots; \mathbf{v}_{k,L_k}], \quad (4)$$

i.e. $\text{rank} \tilde{\mathbf{V}}_k = L_k \leq R_k = \text{rank} \mathbf{V}_k$. Numbers L_k (and particular selection of $\tilde{\mathbf{V}}_k$) are defined during the Rank Adaptation problem that, along with Scheduler, is solved before precoding. For the Rank adaptation problem, we refer for example to [23] and in what follows we consider L_k , $\tilde{\mathbf{V}}_k$ already chosen.

2.2. Precoding Matrices

The *precoding* matrix \mathbf{W} is responsible for the beamforming from the base station to the users [10]. The linear methods for precoding do the following. Firstly, the linear solutions obtain singular value decomposition for each user $\mathbf{H}_k = \mathbf{U}_k^H \mathbf{S}_k \mathbf{V}_k \in \mathbb{C}^{R_k \times T}$ (Lemma 2.1) and take the first L_k singular vectors $\tilde{\mathbf{V}}_k \in \mathbb{C}^{L_k \times T}$ which attend to the first L_k greatest singular values [33]. All these matrices are concatenated to the one matrix $\tilde{\mathbf{V}} \in \mathbb{C}^{L \times T}$, which is used as the main building block of these precoding constructions. Finally, the precoding matrix is constructed from the obtained singular vectors. We describe linear methods for constructing a precoding matrix.

We are considering precoding matrices in the following form:

$$\mathbf{W} = \mathbf{W}' \mathbf{P}, \quad \mathbf{W}' = \mathbf{W}'(\tilde{\mathbf{V}}), \quad (5)$$

where $\tilde{\mathbf{V}}$ is taken from the specific SVD decomposition from Lemma 2.1 and \mathbf{P} is a diagonal matrix of power allocation.

Let us repeat some known algorithms of precoding that are usually considered as baseline or reference. A *Maximum Ratio Transmission* (MRT) [28], *Zero-Forcing* (ZF) [40], *Regularized Zero-Forcing* (RZF), [38] and *Adaptive Regularized Zero-Forcing* [7] precoding algorithms are defined as follows :

$$\mathbf{W}_{MRT} = \tilde{\mathbf{V}}^H \mathbf{P} \quad (6)$$

$$\mathbf{W}_{ZF} = \tilde{\mathbf{V}}^\dagger \mathbf{P}, \quad \tilde{\mathbf{V}}^\dagger := \tilde{\mathbf{V}}^H (\tilde{\mathbf{V}} \tilde{\mathbf{V}}^H)^{-1} \quad (7)$$

$$\mathbf{W}_{RZF} = \tilde{\mathbf{V}}^H (\tilde{\mathbf{V}} \tilde{\mathbf{V}}^H + \lambda \mathbf{I})^{-1} \mathbf{P} \quad (8)$$

$$\mathbf{W}_{ARZF} = \tilde{\mathbf{V}}^H (\tilde{\mathbf{V}} \tilde{\mathbf{V}}^H + \lambda \mathbf{S}^{-2})^{-1} \mathbf{P}. \quad (9)$$

2.3. Detection Matrices

After precoding and transmission, on the side of UE k , we have to choose a detection matrix $\mathbf{G}_k \in \mathbb{C}^{L_k \times R_k}$, which takes into account the rank of UE L_k . The way the UE performs detection strongly affects overall performance, and different detection algorithms require different optimal precoding matrices (see [19], where precoding is chosen as a function of the detection matrix). The best way would be to consistently choose precoding and detection, but this is hardly possible due to the distributed nature of wireless communication. However, there are ideas on how to set up a precoding matrix, assuming a specific detection method on the UE side in the transmitter [32]. We do not consider such an approach in our work, although it can be used to further improve our main proposal.

We assume the *effective channel* matrix $\mathbf{A}_k = \mathbf{H}_k \mathbf{W}_k$ to be calculated on the UE side. The Minimum Mean Square Error (*MMSE*) detection for the user k , where $\lambda \geq 0$ is the regularization value [25, 39], performs as follows:

$$\mathbf{G}_k^{MMSE}(\lambda) = (\mathbf{A}_k^H \mathbf{A}_k + \lambda \mathbf{I})^{-1} \mathbf{A}_k^H \quad (10)$$

In this paper, priority is given to the *MMSE-Interference-Rejection-Combiner* (*MMSE-IRC*) detection [30]:

$$\mathbf{G}_k^{IRC}(\lambda) = \mathbf{A}_k^H (\mathbf{A}_k^H \mathbf{A}_k + \mathbf{R}_{uu}^k + \lambda \mathbf{I})^{-1}. \quad (11)$$

And covariance matrix \mathbf{R}_{uu}^k of total intra user interference:

$$\mathbf{R}_{uu}^k = \mathbf{H}_k (\mathbf{W} \mathbf{W}^H - \mathbf{W}_k \mathbf{W}_k^H) \mathbf{H}_k^H. \quad (12)$$

To conduct analytical calculations, we assume virtual Conjugate Detection (*CD*) in the following form [7]:

$$\mathbf{G}_k^C = \mathbf{P}_k^{-1} \tilde{\mathbf{S}}_k^{-1} \tilde{\mathbf{U}}_k = \mathbf{P}_k^{-1} \hat{\mathbf{G}}_k^C \in \mathbb{C}^{L_k \times R_k}, \quad (13)$$

where \mathbf{P}_k is a corresponding to k -th user sub-matrix of matrix \mathbf{P} in equation (5) .

2.4. Quality Measures

We measure the quality of precoding using well-known functions such as Signal-to-Interference-and-Noise-Ratio (*SINR*) [37] and Spectral Efficiency (*SE*) [36]. These functions are based not on the actual sending symbols $\mathbf{x} \in \mathbb{C}^{L \times 1}$, but some distribution of them [3]. Thus, we get the common function for all assumed symbols, which can be sent using the specified precoding matrix. We denote \mathcal{L}_k as the set of symbols for k -th user. The *SINR* function is defined as:

$$SINR_l(\mathbf{W}, \mathbf{H}_k, \mathbf{g}_l, \sigma^2) := \frac{|\mathbf{g}_l \mathbf{H}_k \mathbf{w}_l|^2}{\sum_{i \neq l}^L |\mathbf{g}_l \mathbf{H}_k \mathbf{w}_i|^2 + \sigma^2 \|\mathbf{g}_l\|^2}, \quad \forall l \in \mathcal{L}_k, \quad (14)$$

According to the paper [16], the *effective SINR* for user k is calculated through the *SINR* at each layer of each RB and as follows. Functions $\beta = \beta(MCS)$ and $MCS \approx f(SINR^{eff})$ are table-defined (see e.g. Table 2 for $\beta(MCS)$). This model was

considered in [20]. Assuming only one RB we can define $SINR^{eff}$ as a self-consistent solution of the following system:

$$SINR_{\beta,k}^{eff}(\mathbf{W}, \mathbf{H}_k, \mathbf{G}_k, \sigma^2) = -\beta \ln \left(\frac{1}{L_k} \sum_{j=1}^{L_k} \exp \left\{ - \frac{SINR_l(\mathbf{W}, \mathbf{H}_k, \mathbf{g}_l, \sigma^2)}{\beta} \right\} \right), \quad \forall l \in \mathcal{L}_k, \quad (15)$$

To get the SE function we apply Shannon's formula over all effective user SINRs (37):

$$SE(\mathbf{W}, \mathbf{H}, \mathbf{G}, \sigma^2) = \sum_{k=1}^K L_k \log_2(1 + SINR_{\beta,k}^{eff}(\mathbf{W}, \mathbf{H}_k, \mathbf{G}_k, \sigma^2)) \rightarrow \max_{\mathbf{W}} \quad (16)$$

2.5. Problem Statement

We consider the channel model in the form (1) that particularly means exact measurements of the channel. To further simplify the problem we suppose detection policy $\mathbf{G} = \mathbf{G}(\mathbf{H}, \mathbf{W})$ to be a known function, moreover we assume Conjugate Detection (13) that simplifies the channel model to (27). Based on this channel model we calculate $SINR$ of transmitted symbols by (14) and effective $SINR$ of UE, which can be approximately calculated by (15) and (37). We denote the total power of the system as P and assume that the sent vector must be a unit norm: $\mathbb{E}[\mathbf{x}\mathbf{x}^H] = \mathbf{I}_L$.

The *total power constraint* and the more realistic *per-antenna power constraints* (see [4]) impose the following conditions on the precoding matrix. Since case $\mathbf{W} = \mathbf{W}'(\mathbf{V})\mathbf{P}$ is considered in this paper, conditions read:

$$(a) \quad \|\mathbf{W}'\mathbf{P}\|^2 \leq P, \quad \text{or} \quad (b) \quad \|\mathbf{w}'_t \mathbf{p}\|^2 \leq P/T, \quad t = 1, \dots, T. \quad (17)$$

Where $\mathbf{P} = \text{diag}(\mathbf{p}) = \text{diag}(\sqrt{p_1} \dots \sqrt{p_L}) = \text{diag}\left(\frac{\sqrt{\rho_1}}{\|\mathbf{w}'_1\|} \dots \frac{\sqrt{\rho_L}}{\|\mathbf{w}'_L\|}\right)$ is power allocation matrix and P is total power of base station. **The goal is to find a precoding matrix that maximizes SE (16) given the power constraints:**

$$SE(\mathbf{P}) = SE(\mathbf{W}'\mathbf{P}, \mathbf{H}, \mathbf{G}(\mathbf{H}, \mathbf{W}'\mathbf{P}), \sigma^2) \rightarrow \max_{\mathbf{P}}, \quad \text{subject to (17) (a) or (b).} \quad (18)$$

3. Simplifications of the Problem

3.1. Asymptotic Diagonalization Property of Precoding

Definition 3.1. Let us denote $\lambda = \frac{\sigma^2}{P} \rightarrow 0$, and $\mathbf{P} > 0$ is some diagonal matrix. Define the property of **asymptotic diagonalization of $\tilde{\mathbf{V}}$** as $\lambda \rightarrow 0$ of precoding matrix as follows:

$$\tilde{\mathbf{V}}\mathbf{W} = \begin{pmatrix} \tilde{\mathbf{V}}_1 \\ \tilde{\mathbf{V}}_2 \\ \dots \\ \tilde{\mathbf{V}}_K \end{pmatrix} \cdot (\mathbf{W}_1, \mathbf{W}_2 \dots \mathbf{W}_K) = \mathbf{P} + \mathcal{O}(\lambda), \quad \text{i.e. } \tilde{\mathbf{V}}\mathbf{W} \sim \mathbf{P}, \text{ as } \lambda \rightarrow 0 \quad (19)$$

Precoding algorithms: ZF (7), RZF (8), and ARZF (9) satisfy the property (19). This can be easily shown with the following Lemma (it is similar to [7, Lemma 2]).

Lemma 3.2. *Consider square invertible complex matrices \mathbf{M} and \mathbf{N} of the same size and rank. For any $0 < \lambda \ll 1$ and $\det \mathbf{M} \neq 0$ the following matrix identity is true: $(\mathbf{M} + \lambda \mathbf{N})^{-1} = \mathbf{M}^{-1} - \lambda \mathbf{M}^{-1} \mathbf{N} \mathbf{M}^{-1} + \mathcal{O}(\lambda^2) = \mathbf{M}^{-1} + \mathcal{O}(\lambda)$.*

Proof.

$$\mathbf{F}(\lambda) = (\mathbf{M} + \lambda \mathbf{N})^{-1}, \text{ and } \mathbf{F}'(\lambda) = -(\mathbf{M} + \lambda \mathbf{N})^{-1} \mathbf{N} (\mathbf{M} + \lambda \mathbf{N})^{-1} \quad (20)$$

$$\mathbf{F}(\lambda) = \mathbf{F}(0) + \mathbf{F}'(0)\lambda + \mathcal{O}(\lambda^2), \text{ where } \mathbf{F}(0) = \mathbf{M}^{-1}, \text{ and } \mathbf{F}'(0) = -\mathbf{M}^{-1} \mathbf{N} \mathbf{M}^{-1} \quad (21)$$

$$(\mathbf{M} + \lambda \mathbf{N})^{-1} = \mathbf{M}^{-1} - \lambda \mathbf{M}^{-1} \mathbf{N} \mathbf{M}^{-1} + \mathcal{O}(\lambda^2) = \mathbf{M}^{-1} + \mathcal{O}(\lambda) \quad (22)$$

□

For channel singular values $\tilde{\mathbf{V}}$ such that matrix $\tilde{\mathbf{V}} \tilde{\mathbf{V}}^H$ has a full rank, using Lemma 3.2 for the algorithms ZF (7), RZF (8) and ARZF (9) we obtain:

$$\tilde{\mathbf{V}} \mathbf{W}_{ZF} = \tilde{\mathbf{V}} \tilde{\mathbf{V}}^H (\tilde{\mathbf{V}} \tilde{\mathbf{V}}^H)^{-1} \mathbf{P} = \mathbf{P} \quad (23)$$

$$\tilde{\mathbf{V}} \mathbf{W}'_{RZF} = \tilde{\mathbf{V}} \tilde{\mathbf{V}}^H (\tilde{\mathbf{V}} \tilde{\mathbf{V}}^H + \lambda \mathbf{I})^{-1} \mathbf{P} = \mathbf{P} + \mathcal{O}(\lambda) \quad (24)$$

$$\tilde{\mathbf{V}} \mathbf{W}'_{ARZF} = \tilde{\mathbf{V}} \tilde{\mathbf{V}}^H (\tilde{\mathbf{V}} \tilde{\mathbf{V}}^H + \lambda \mathbf{S})^{-1} \mathbf{P} = \mathbf{P} + \mathcal{O}(\lambda) \quad (25)$$

Thus, precodings ZF (7), RZF (8), and ARZF (9) satisfy property (19).

Remark 1. In this case, matrix \mathbf{P} of definition (19) coincides with matrix \mathbf{P} of Conjugate Detection (13).

3.2. The Similarity of Conjugate Detection and MMSE-IRC

In this section, we prove the similarity of MMSE-IRC (11) [30] and Conjugate Detection (CD) (13) [7]. Detection CD does not depend on precoding and allows to significantly simplify the considered problem (18). First, we prove some useful properties about CD (compare with [7, Theorem 1]).

Lemma 3.3. *The detection matrix \mathbf{G} is \mathbf{G}^C (Conjugate Detection) if and only if it satisfies the following property:*

$$\mathbf{G} = \mathbf{G}^C \Leftrightarrow \mathbf{G} \mathbf{H} = \mathbf{P}^{-1} \tilde{\mathbf{V}} \Leftrightarrow \forall k : \mathbf{G}_k \mathbf{H}_k = \mathbf{P}_k^{-1} \tilde{\mathbf{V}}_k, \quad (26)$$

where \mathbf{P} is uniquely defined in (19), and the system model equation (1) takes the form

$$\mathbf{r} = \tilde{\mathbf{V}} \mathbf{W} \mathbf{x} + \tilde{\mathbf{n}}, \quad \tilde{\mathbf{n}} := \mathbf{P}^{-1} \tilde{\mathbf{S}}^{-1} \tilde{\mathbf{U}} \mathbf{n}. \quad (27)$$

Proof. Necessity. Using Lemma (2.1) we can write

$$\begin{aligned} \mathbf{G}^C \mathbf{H} &= \mathbf{P}^{-1} \tilde{\mathbf{S}}^{-1} \tilde{\mathbf{U}} \mathbf{U}^H \mathbf{S} \mathbf{V} = \mathbf{P}^{-1} \tilde{\mathbf{S}}^{-1} [\mathbf{I} \mid \mathbf{O}] \mathbf{S} \mathbf{V} = \\ &= \mathbf{P}^{-1} \tilde{\mathbf{S}}^{-1} \left[\begin{array}{c|c} \tilde{\mathbf{S}} & \mathbf{O} \\ \hline \mathbf{O} & \mathbf{O} \end{array} \right] \mathbf{V} = \mathbf{P}^{-1} \tilde{\mathbf{S}}^{-1} \tilde{\mathbf{S}} \tilde{\mathbf{V}} = \mathbf{P}^{-1} \tilde{\mathbf{V}}, \quad (28) \end{aligned}$$

which immediately leads to (27).

Sufficiency. Assume that (26) holds, then $\tilde{\mathbf{V}} = \mathbf{P} \mathbf{G} \mathbf{H}$, since the matrix $\mathbf{P} > \mathbf{O}$. Then, $\forall \mathbf{v} \in \tilde{\mathbf{V}}$ expansion of vector \mathbf{v} in basis \mathbf{H} is unique. The elements of the matrix $\mathbf{P} \mathbf{G}$ are the coefficients of this expansion. Therefore, matrix \mathbf{G} with the property (26) is unique.

The last equivalence in (26) is true due to the block-diagonality of the matrix \mathbf{G} . \square

Theorem 3.4. *In assumption that \mathbf{H}_k has the full rank and precoding \mathbf{W} has property (19), detection $\mathbf{G}^{IRC}(\lambda)$ (11) asymptotically equals to \mathbf{G}^C (13), in other words $\mathbf{G}^{IRC}(\lambda) \sim \mathbf{G}^C$ as $\lambda \rightarrow 0$.*

Proof. We need the following consequence of the (19) property:

$$\mathbf{W} \mathbf{W}^H \tilde{\mathbf{V}}_k^H = \left(\sum_{u=1}^K \mathbf{W}_u \mathbf{W}_u^H \right) \tilde{\mathbf{V}}_k^H \sim \mathbf{W}_k \mathbf{W}_k^H \tilde{\mathbf{V}}_k^H \sim \mathbf{W}_k \mathbf{P}_k \quad (29)$$

Taking into account the form of \mathbf{R}_{uu}^k we can rewrite [9]:

$$\begin{aligned} \mathbf{G}_k^{IRC}(\lambda) &= (\mathbf{H}_k \mathbf{W}_k)^H (\mathbf{H}_k \mathbf{W}_k (\mathbf{H}_k \mathbf{W}_k)^H + \mathbf{R}_{uu}^k + \lambda \mathbf{I})^{-1} = \\ &= (\mathbf{H}_k \mathbf{W}_k)^H (\mathbf{H}_k \mathbf{W}_k (\mathbf{H}_k \mathbf{W}_k)^H + \mathbf{H}_k (\mathbf{W} \mathbf{W}^H - \mathbf{W}_k \mathbf{W}_k^H) \mathbf{H}_k^H + \lambda \mathbf{I})^{-1} = \\ &= (\mathbf{H}_k \mathbf{W}_k)^H (\mathbf{H}_k \mathbf{W} (\mathbf{H}_k \mathbf{W})^H + \lambda \mathbf{I})^{-1}. \quad (30) \end{aligned}$$

Using (26), (29), Lemma 3.3 in the case $\lambda \rightarrow 0$ we obtain:

$$\begin{aligned} \mathbf{G}_k^C &= \mathbf{I} \mathbf{G}_k^C \mathbf{I} = \mathbf{P}_k^{-1} \mathbf{P}_k \mathbf{G}_k^C (\mathbf{H}_k \mathbf{W} (\mathbf{H}_k \mathbf{W})^H) (\mathbf{H}_k \mathbf{W} (\mathbf{H}_k \mathbf{W})^H)^{-1} = \{Eq. 26\} = \\ &= \mathbf{P}_k^{-1} \tilde{\mathbf{V}}_k \mathbf{W} \mathbf{W}^H \mathbf{H}_k^H (\mathbf{H}_k \mathbf{W} (\mathbf{H}_k \mathbf{W})^H)^{-1} \sim \{Eq. 29\} \sim \\ &\sim \mathbf{W}_k^H \mathbf{H}_k^H (\mathbf{H}_k \mathbf{W} (\mathbf{H}_k \mathbf{W})^H)^{-1} = (\mathbf{H}_k \mathbf{W}_k)^H (\mathbf{H}_k \mathbf{W} (\mathbf{H}_k \mathbf{W})^H)^{-1} \sim \mathbf{G}_k^{IRC}. \quad (31) \end{aligned}$$

\square

Remark 2. The introduced *CD* detection is speculative: it hardly can be implemented in practice. UE measures $\mathbf{H}_k \mathbf{W}_k$ via pilot signals instead of \mathbf{H}_k . Nonetheless, it is very useful for theoretical research. Moreover, the asymptotic behavior of *MMSE* and *MMSE-IRC* detection is similar to that of *CD* (Sec. 3.2). Particularly, if precoding \mathbf{W} is Zero-Forcing (7) and the noise power is zero ($\sigma^2 = 0$), then $\mathbf{G}^{IRC}(\lambda) = \mathbf{G}^C$; if, additionally, precoding has the full rank, then $\mathbf{G}^{MMSE}(\lambda) = \mathbf{G}^C$.

Remark 3. Lemma 3.3 shows that the assumption that UEs use *CD* on their side sufficiently simplifies the initial problem, decreases its dimensions, and allows notation to be uniform. Namely, we can work with *user layers* of shapes L_k and L instead of considering *user antennas* space. Note also that for precoding it is sufficient to only

perform Partial SVD of the channel $\mathbf{H}_k \in \mathbb{C}^{R_k \times T}$, keeping just the first L_k singular values and vectors for each user k :

$$\mathbf{H}_k \approx \tilde{\mathbf{U}}_k^H \tilde{\mathbf{S}}_k \tilde{\mathbf{V}}_k. \quad (32)$$

Based on this, in what follows we can omit the tilde and write $\mathbf{U}_k, \mathbf{S}_k, \mathbf{V}_k$ instead of $\tilde{\mathbf{U}}_k, \tilde{\mathbf{S}}_k, \tilde{\mathbf{V}}_k$ correspondingly.

3.3. Effective SINR Models

In this subsection we compare two models of effective sinr from [7, 16, 20]. We define an *interference-correlation matrix* as $\mathbf{C} = \mathbf{V}\mathbf{V}^H - \mathbf{I}$. We assume user correlation to be low compared to noise power, which means $\|\mathbf{C}\| = \mathcal{O}(\lambda)$, where $\lambda = \frac{\sigma^2}{P}$ is the noise-power ratio.

Remark 4. In real networks, the set of UEs is chosen by Scheduler and the number of layers of each UE is chosen to be fixed by the Rank Selection algorithm. Both Scheduler and Rank Selection methods provide $\|\mathbf{C}\| = \mathcal{O}(\lambda)$.

Lemma 3.5. *For precoding $\mathbf{W} = \mathbf{W}'\mathbf{P}$ satisfying the property (19) and inference-correlation matrix $\mathbf{C} = \mathbf{V}\mathbf{V}^H - \mathbf{I}$ satisfying $\|\mathbf{C}\| = \mathcal{O}(\lambda)$, is the noise-power ratio, it is asymptotically true that $\mathbf{G}^C \mathbf{H}\mathbf{W} = (1 - \lambda)\mathbf{I} + \mathcal{O}(\lambda^2)$.*

Proof.

$$\begin{aligned} \mathbf{V}\mathbf{W}' &= \mathbf{V}\mathbf{V}^H(\mathbf{V}\mathbf{V}^H + \lambda\mathbf{I})^{-1} = \{\text{Lemma 3.2}\} = \mathbf{V}\mathbf{V}^H((\mathbf{V}\mathbf{V}^H)^{-1} - \lambda(\mathbf{V}\mathbf{V}^H)^{-2} + \mathcal{O}(\lambda^2)) = \\ &= \mathbf{I} - \lambda(\mathbf{V}\mathbf{V}^H)^{-1} + \mathcal{O}(\lambda^2) = \mathbf{I} - \lambda(\mathbf{C} + \mathbf{I})^{-1} + \mathcal{O}(\lambda^2) = \mathbf{I} - \lambda(\mathbf{I} + \mathcal{O}(\|\mathbf{C}\|)) + \mathcal{O}(\lambda^2) = \\ &= (1 - \lambda)\mathbf{I} + \lambda\mathcal{O}(\|\mathbf{C}\|) + \mathcal{O}(\lambda^2) = \{\|\mathbf{C}\| = \mathcal{O}(\lambda)\} = (1 - \lambda)\mathbf{I} + \mathcal{O}(\lambda^2) \end{aligned} \quad (33)$$

$$\begin{aligned} \mathbf{G}^C \mathbf{H}\mathbf{W} &= \{\text{Lemma 3.3}\} = \mathbf{P}^{-1}\mathbf{V}\mathbf{W} = \mathbf{P}^{-1}\mathbf{V}\mathbf{W}'\mathbf{P} = \{\text{Eq. 33}\} = \\ &= \mathbf{P}^{-1}(1 - \lambda)\mathbf{I}\mathbf{P} + \mathbf{P}^{-1}\mathcal{O}(\lambda^2)\mathbf{P} = (1 - \lambda)\mathbf{I} + \mathcal{O}(\lambda^2) \end{aligned} \quad (34)$$

□

Using Lemma 3.5 we immediately get the following

Theorem 3.6. *For precoding \mathbf{W} satisfying the property (19) and inference-correlation matrix $\mathbf{C} = \mathbf{V}\mathbf{V}^H - \mathbf{I}$ satisfying $\|\mathbf{C}\| = \mathcal{O}(\lambda)$, where $\lambda = \frac{\sigma^2}{P}$ is the noise-power ratio, formula for SINR (14) in the case of \mathbf{G}^C (13) detection will take the asymptotic form:*

$$\text{SINR}_l(\mathbf{W}, \mathbf{H}_k, \mathbf{g}_l^C, \sigma^2) \sim \frac{p_l s_l^2}{\sigma^2} \quad (35)$$

Proof.

$$\begin{aligned}
SINR_l(\mathbf{W}, \mathbf{H}_k, \mathbf{g}_l^C, \sigma^2) &:= \frac{|\mathbf{g}_l^C \mathbf{H}_k \mathbf{w}_l|^2}{\sum_{i=1, i \neq l}^L |\mathbf{g}_l^C \mathbf{H}_k \mathbf{w}_i|^2 + \sigma^2 \|\mathbf{g}_l^C\|^2} = \{ \text{Lemma 3.5} \} = \\
&= \frac{1 - \lambda + \mathcal{O}(\lambda^2)}{\mathcal{O}(\lambda^2) + \frac{\sigma^2}{p_l s_l^2}} = \frac{1 - \frac{\sigma^2}{P} + \mathcal{O}\left(\frac{\sigma^4}{P^2}\right)}{\mathcal{O}\left(\frac{\sigma^4}{P^2}\right) + \frac{\sigma^2}{p_l s_l^2}} \sim \frac{p_l s_l^2}{\sigma^2} \quad (36)
\end{aligned}$$

□

In theoretical calculations, model (15) is extremely inconvenient. To simplify the formula of *effective SINR* (15), we average his L_k per-symbol *SINRs* (14) by the geometric mean, where \mathcal{L}_k denotes the set of symbols for k -th user:

$$SINR_k^{eff}(\mathbf{W}, \mathbf{H}_k, \mathbf{G}_k, \sigma^2) = \left(\prod_{l \in \mathcal{L}_k} SINR_l(\mathbf{W}, \mathbf{H}_k, \mathbf{g}_l, \sigma^2) \right)^{\frac{1}{L_k}}, \quad \forall l \in \mathcal{L}_k, \quad (37)$$

To justify the close relationship of the various *SINR* averaging (15) and (37), Fig. 5 shows the dependencies of $SINR_{eff}(dB)$ for a user with four antennas. The x axis is the sum $SINR_1(dB) + SINR_2(dB) + SINR_3(dB) + SINR_4(dB)$. Fig. 5 shows the comparison of effective *SINR* in the form of the geometric mean and the form of QAM-64 and QAM-256. Differences between different effective *SINRs* can be more than five decibels, but points with very different *SINRs* do not exist in practice. The dependence of the effective *SINR* deviation on the difference between the minimum and maximum *SINR* (Fig. 6) proves this fact.

For precoding \mathbf{W} satisfying the property (19) and from the formula for *SINR* (35) with a *CD* using the geometric mean effective *SINR* model (37), we can write the *SINR* for the k th user as follows:

$$SINR_{eff}^k(\tilde{\mathbf{S}}_k, \mathbf{P}_k, \sigma^2) = \frac{1}{\sigma^2} \sqrt[L_k]{\prod_{l=1}^{L_k} (s_l^2 p_l)}. \quad (38)$$

The formula (38) reflects the channel quality for the specified user without considering other users. The value of $SINR_{eff}^k(\tilde{\mathbf{S}}_k, \mathbf{P}_k, \sigma^2)$ depends on the singular values $\tilde{\mathbf{S}}_k \in \mathbb{R}^{L_k \times L_k}$ (related to matrices $\mathbf{H}_k \in \mathbb{C}^{R_k \times T}$), the transmitted power \mathbf{P}_k and noise σ^2 . This function will be used in theoretical calculations due to its simplicity.

3.4. Sum Spectral Efficiency

For any $x \gg 1$ it is true that: $\log(1 + x) = \log x + O(x^{-1})$, and so

$$\begin{aligned}
SE(\mathbf{W}, \mathbf{V}, \sigma^2) &= \sum_{k=1}^K L_k \log_2(1 + SINR_k^{eff}(\mathbf{W}, \mathbf{V}_k, \mathbf{S}_k, \sigma^2)) = \\
&= \sum_{k=1}^K L_k \log_2(SINR_k^{eff}(\mathbf{W}, \mathbf{V}_k, \mathbf{S}_k, \sigma^2)) + \sum_{k=1}^K \mathcal{O}(SINR_k^{eff(-1)}(\mathbf{W}, \mathbf{V}_k, \mathbf{S}_k, \sigma^2)) \quad (39)
\end{aligned}$$

We simplify the initial optimization problem by maximization of its leading term:

$$\begin{aligned} \sum_{k=1}^K L_k \log_2(SINR_k^{eff}(\mathbf{W}, \mathbf{V}_k, \mathbf{S}_k, \sigma^2)) &= \sum_{k=1}^K L_k \log_2 \left(\prod_{l \in \mathcal{L}_k} SINR_l(\mathbf{W}, \mathbf{H}_k, \mathbf{g}_l, \sigma^2, P) \right)^{\frac{1}{L_k}} = \\ &= \sum_{k=1}^K \log_2 \prod_{l \in \mathcal{L}_k} SINR_l(\mathbf{W}, \mathbf{H}_k, \mathbf{g}_l, \sigma^2, P) \rightarrow \max_{\mathbf{P}} \quad (40) \end{aligned}$$

These problems are not equivalent, although their solutions are close to each other.

If we calculate W by ZF algorithm (that gives zero interference) $SINR$ are as follows

$$SINR_l(\mathbf{W}, \mathbf{v}_l, s_l, \sigma^2) = \{\text{Zero-Forcing Algorithm}\} = \frac{s_l^2}{\sigma^2} p_l \quad (41)$$

and maximization of the leading term gives

$$\begin{aligned} \sum_{k=1}^K \log_2 \prod_{l \in \mathcal{L}_k} SINR_l(\mathbf{W}, \mathbf{v}_l, s_l, \sigma^2) &= \sum_{k=1}^K \log_2 \prod_{l \in \mathcal{L}_k} \frac{s_l^2}{\sigma^2} p_l = \sum_{k=1}^K \log_2 \prod_{l \in \mathcal{L}_k} \frac{s_l^2}{\sigma^2} \prod_{l \in \mathcal{L}_k} p_l = \\ &= \sum_{j=1}^K \log_2 \prod_{l \in \mathcal{L}_k} s_l^2 - \sum_{j=1}^K \log_2 \prod_{l \in \mathcal{L}_k} \sigma^2 + \sum_{j=1}^K \log_2 \prod_{l \in \mathcal{L}_k} p_l \rightarrow \max_{\mathbf{P}} \quad (42) \end{aligned}$$

Finally, we can reduce tasks (18) (a) and (b) to the following problems:

$$\sum_{k=1}^K \log_2 \prod_{l \in \mathcal{L}_k} p_l = \log_2 \prod_{l=1}^L p_l \rightarrow \max_{\mathbf{P}}, \quad \text{s.t. } \|\mathbf{W}\|^2 \leq P. \quad (43)$$

4. Solutions of the Problem

According to [4, sec. 7] we consider equal transmit power strategy for all K users. Such power allocation gives the maximum for a reasonable lower bound on the SE (16) under some feasible assumptions. Although this Power allocation is not optimal, these heuristics provide a good sub-optimal solution.

4.1. Simplified with Total Power Constraints

Theorem 4.1. *If \mathbf{W} satisfies to the property (19) and $G = G_C$, assuming model (15) of effective $SINR$, the equal PA (all $\|\mathbf{w}_l\|$ is equal, namely, $p_l = P/L$) asymptotically provides maximum to the first optimization problem:*

$$U = \sum_n SE_n \rightarrow \max, \quad \|\mathbf{W}\|^2 \leq P. \quad (44)$$

Proof. Using asymptotic $\ln(1+SINR) = \ln(SINR)(1+O(\varepsilon))$ for large $SINR$, conjugate detection, $SINR$ estimation (41) for ZF algorithm and considering coordinates ρ we

get first optimization problem (18):

$$\prod_{l=1}^L \rho_l \rightarrow \max_{\rho_1 \dots \rho_L}, \quad \text{s.t.} \quad \sum_{l=1}^L \|\mathbf{w}'_l\|^2 \frac{\rho_l}{\|\mathbf{w}'_l\|^2} = \sum_{l=1}^L \rho_l \leq P. \quad (45)$$

It is an optimization problem of the maximal volume of the box with predefined lengths of edges which solution is

$$\forall l : \rho_l = P/L, \quad \text{and} \quad p_l = \frac{P/L}{\|\mathbf{w}'_l\|^2} \quad (46)$$

□

Remark 5. The original function (16), (37) asymptotically reaches its maximum at the solution of the simplified problem (46).

4.2. QAM Modulation and Total Power Constraints

By analogy with the formulas (39 and 40) we can calculate Spectral efficiency using QAM model (15), where parameter β_k for each $k = 1 \dots K$ depends on given MCS and therefore depends on the precoding matrix, in particular on power allocation variables p_l for all $l = 1 \dots L$:

$$\begin{aligned} SE(\mathbf{W}, \mathbf{H}, \sigma^2) &= \sum_{k=1}^K L_k \ln(1 + SINR_k^{eff}) = \\ &= - \sum_{k=1}^K L_k \ln \left(1 - \beta_k \log \left(\frac{1}{L_k} \sum_{j=1}^{L_k} \exp \left(- \frac{SINR_{kj}}{\beta_k} \right) \right) \right) \end{aligned} \quad (47)$$

The function (47) is discontinuous. Nevertheless, if we fix β_k for all $k = 1 \dots K$, this function becomes smooth from p_k . For example, we can take β_k from point P_1 as $(p_1)_i = \frac{P/L}{\|\mathbf{w}'_i\|^2}$. Next, write $SINR$ similar to the formula (35) without interference as $SINR_{kl} = \frac{p_l}{\|\mathbf{g}_l\|^2 \sigma^2}$ (g_l does not depend on p_l). We can write Lagrangian for the problem 18 (a):

$$\mathcal{L} = - \sum_{k=1}^K L_k \ln \left(1 - \beta_l \log \left(\frac{1}{L_k} \sum_{j=1}^{L_k} \exp \left(- \frac{p_j}{\sigma^2 \beta_l \|\mathbf{g}_j\|^2} \right) \right) \right) + \lambda_1 \left(\sum_{l=1}^L (\|\mathbf{w}'_l\|^2 p_l) - P \right) \quad (48)$$

And its partial derivatives concerning p_l .

$$\mathcal{L}'_{p_l} = - \frac{\frac{1}{\beta_l \sigma^2 \|\mathbf{g}_l\|^2} x_l}{(1 - \beta_l \ln(X_k)) X_k} + \sum_{t=1}^T (\lambda_t |w'_{tl}|^2) \quad (49)$$

There $x_l = \exp \left(- \frac{p_l}{\beta_l \sigma^2 \|\mathbf{g}_l\|^2} \right)$ and $X_k = \frac{1}{L_k} \sum_{i=1}^{L_k} \exp \left(- \frac{p_i}{\beta_l \sigma^2 \|\mathbf{g}_i\|^2} \right)$

We can write Karush–Kuhn–Tucker conditions:

$$\begin{cases} \mathcal{L}'_{p_l} = 0, \quad l = 1 \dots L \\ \lambda_1 \left(\sum_{l=1}^L (\|\mathbf{w}'_l\|^2 p_l) - P \right) = 0, \\ \lambda_1 \geq 0 \end{cases} \quad (50)$$

And its solution is (see proof in Appendix):

$$p_l = p_l(\|\mathbf{w}'_1\|, \dots, \|\mathbf{w}'_L\|) = -\ln(x_l) \beta_k \sigma^2 \|\mathbf{g}_l\|^2 = -\beta_k \sigma^2 \|\mathbf{g}_l\|^2 \ln \left(f_k \frac{\|\mathbf{g}_l\|^2 \|\mathbf{w}'_l\|^2}{\frac{1}{L_k} \sum_{s=1}^{L_k} \|\mathbf{g}_s\|^2 \|\mathbf{w}'_s\|^2} \right) \quad (51)$$

$$f_k = \exp \left(\frac{1}{\beta_k} \right) \exp \left(1 - \frac{P + \sum_{l=1}^L \sigma^2 \|\mathbf{g}_l\|^2 \|\mathbf{w}'_l\|^2 \left(\beta_k \ln \left(\frac{\|\mathbf{g}_l\|^2 \|\mathbf{w}'_l\|^2}{\frac{1}{L_k} \sum_{s=1}^{L_k} \|\mathbf{g}_s\|^2 \|\mathbf{w}'_s\|^2} \right) + 1 \right)}{\frac{1}{L_k} \sum_{l=1}^{L_k} (\beta_k \sigma^2 \|\mathbf{g}_l\|^2 \|\mathbf{w}'_l\|^2) \sum_{l=1}^L \frac{\|\mathbf{g}_l\|^2 \|\mathbf{w}'_l\|^2}{\frac{1}{L_k} \sum_{s=1}^{L_k} (\beta_k \|\mathbf{g}_s\|^2 \|\mathbf{w}'_s\|^2)}} \right) \quad (52)$$

4.3. Simplified with Per-Antenna Power Constraints

Theorem 4.2. *If \mathbf{W} satisfies to the property (19) and $G = G_C$, assuming model (15) of effective SINR, we can find a strict asymptotic solution of the second optimization problem*

$$U = \sum_n SE_n \rightarrow \max, \quad \|\mathbf{w}_t\|^2 \leq \frac{P}{T}, \quad t = 1 \dots T. \quad (53)$$

by solving the system of equations.

Proof. The problem (18) (b) can be reduced to a task

$$\sum_{l=1}^L \log(p_l) \rightarrow \max_{\mathbf{P}}, \quad \text{subject to} \quad \sum_{l=1}^L (|w'_{tl}|^2 p_l) \leq \frac{P}{T} \quad \forall t = 1 \dots T \quad (54)$$

To solve it, we can use the Karush–Kuhn–Tucker conditions. Lagrangian has the form

$$\mathcal{L} = - \sum_{l=1}^L \log(p_l) + \sum_{t=1}^T \left(\lambda_t \left(\sum_{l=1}^L (|w'_{tl}|^2 p_l) - \frac{P}{T} \right) \right) \quad (55)$$

If p_l and λ_t are the optimum of the optimization problem, then they satisfy the following conditions

$$\begin{cases} p_l \sum_{t=1}^T |w'_{tl}|^2 \lambda_t = 1, & l = 1 \dots L \\ \lambda_t \left(\sum_{l=1}^L (|w'_{tl}|^2 p_l) - \frac{P}{T} \right) = 0, & t = 1 \dots T \\ \lambda_t \geq 0, & t = 1 \dots T \end{cases} \Leftrightarrow \begin{cases} \mathbf{A}^T \boldsymbol{\lambda} = 1./\mathbf{p} \\ \boldsymbol{\lambda} \cdot (\mathbf{A}\mathbf{p} - \mathbf{1}\frac{P}{T}) = 0 \\ \boldsymbol{\lambda} \geq 0 \end{cases} \quad (56)$$

We take $\mathbf{A} = \{a_{ij} = |w'_{ij}|^2\}$.

For geometric reasons, the original optimization problem has a solution; therefore, there is at least one solution to the system (56).

The resulting system can be solved by brute force on the set of zeroed lambdas. Let's say we zero m lambda. Consider the cases.

1. $m < T - L$, in this case the linear system $\sum_{l=1}^L (|w'_{tl}|^2 p_l) = \frac{P}{T}, t = 1 \dots T$ will be inconsistent since the number of equations is greater than the number of unknowns ($T - m > L$) and the system itself (56) will not have a solution.
2. $m = T - L$, in this case the linear system $\sum_{l=1}^L (|w'_{tl}|^2 p_l) = \frac{P}{T}, t = 1 \dots T$ has exactly one solution, and the system itself (56) has at most one solution.
3. $T - L < m < T - 1$. This case reduces to the system of quadratic equations. If T' is the set of indexes of nonzero lambda and \mathbf{A}' is a matrix consisting of rows of matrix \mathbf{A} corresponding to nonzero lambdas then

$$\begin{cases} \mathbf{A}'^T \boldsymbol{\lambda} = 1./\mathbf{p} \\ (\mathbf{A}'\mathbf{p} - \mathbf{1}\frac{P}{T}) = 0 \end{cases} \Rightarrow \begin{cases} (\mathbf{A}')^\perp (1./\mathbf{p}) = 0 \\ \mathbf{A}'\mathbf{p} = \mathbf{1}\frac{P}{T} \end{cases} \quad (57)$$

Here $\mathbf{A}' \in \mathbb{C}^{(T-m) \times L}$ and $(\mathbf{A}')^\perp \in \mathbb{C}^{(L+m-T) \times L}$ is orthogonal complement to \mathbf{A}'

4. $m = T - 1$, in this case there are one nonzero lambda. Let $\lambda_i \neq 0$ therefore

$$p_l = \frac{1}{\lambda_i |w'_{il}|^2} = \frac{P}{TL |w'_{il}|^2} \quad (58)$$

□

4.4. QAM Modulation and Per-Antenna Power Constraints

In this section we combine two ideas of previous sections. We calculate Spectral efficiency (47) using QAM model (15) and fixed β . Using this, we can write Lagrangian for the problem 18 (b) and its partial derivatives concerning p_l :

$$\mathcal{L} = - \sum_{k=1}^K L_k \ln \left(1 - \beta_l \log \left(\frac{1}{L_k} \sum_{j=1}^{L_k} \exp \left(-\frac{p_j}{\sigma^2 \beta_l \| \mathbf{g}_j \|^2} \right) \right) \right) + \sum_{t=1}^T \lambda_t \left(\sum_{l=1}^L (|w'_{tl}|^2 p_l) - \frac{P}{T} \right) \quad (59)$$

$$\mathcal{L}'_{p_l} = -\frac{\frac{1}{\beta_l \sigma^2 \|\mathbf{g}_l\|^2} x_l}{(1 - \beta_l \ln(X_k)) X_k} + \sum_{t=1}^T (\lambda_t |w'_{tl}|^2) \quad (60)$$

The Karush–Kuhn–Tucker conditions:

$$\begin{cases} \mathcal{L}'_{p_l} = 0, & l = 1 \dots L \\ \lambda_t \left(\sum_{l=1}^L (|w'_{tl}|^2 p_l) - \frac{P}{T} \right) = 0, & t = 1 \dots T \\ \lambda_t \geq 0, & t = 1 \dots T \end{cases} \quad (61)$$

The resulting system can be solved by brute force on the set of zeroed lambdas. Let's say we zero m lambda. Consider the cases.

1. $m < T - L$, in this case the linear system $\sum_{l=1}^L (|w'_{tl}|^2 p_l) = \frac{P}{T}, t = 1 \dots T$ will be inconsistent since the number of equations is greater than the number of unknowns ($T - m \leq L$) and the system itself (61) will not have a solution.
2. $m = T - L$, in this case the linear system $\sum_{l=1}^L (|w'_{tl}|^2 p_l) = \frac{P}{T}, t = 1 \dots T$ has exactly one solution, and the system itself (61) has at most one solution.
3. $T - L < m < T - 1$. If T' is the set of indexes of nonzero lambda then this case reduces to the system of following equations:

$$\begin{cases} \mathcal{L}'_{p_l} = 0 \\ \sum_{l=1}^L (|w'_{tl}|^2 p_l) = \frac{P}{T}, & t \in T' \\ \lambda_t \geq 0, & t \in T' \end{cases} \quad (62)$$

4. $m = T - 1$, in this case there are one nonzero lambda. Let $\lambda_1 \neq 0$ therefore

$$p_l = p_l(|w'_{11}|, \dots, |w'_{1L}|) = -\ln(x_l) \beta_k \sigma^2 \|\mathbf{g}_l\|^2 = -\beta_k \sigma^2 \|\mathbf{g}_l\|^2 \ln \left(f_k \frac{\|\mathbf{g}_l\|^2 |w'_{1l}|^2}{\frac{1}{L_k} \sum_{s=1}^{L_k} \|\mathbf{g}_s\|^2 |w'_{1s}|^2} \right) \quad (63)$$

$$f_k = \exp \left(\frac{1}{\beta_k} \right) \exp \left(1 - \frac{\frac{P}{T} + \sum_{l=1}^L \sigma^2 \|\mathbf{g}_l\|^2 |w'_{1l}|^2 \left(\beta_k \ln \left(\frac{\|\mathbf{g}_l\|^2 |w'_{1l}|^2}{\frac{1}{L_k} \sum_{s=1}^{L_k} \|\mathbf{g}_s\|^2 |w'_{1s}|^2} \right) + 1 \right)}{\frac{1}{L_k} \sum_{l=1}^{L_k} (\beta_k \sigma^2 \|\mathbf{g}_l\|^2 |w'_{1l}|^2) \sum_{l=1}^L \frac{\|\mathbf{g}_l\|^2 |w'_{1l}|^2}{\frac{1}{L_k} \sum_{s=1}^{L_k} (\beta_k \|\mathbf{g}_s\|^2 |w'_{1s}|^2)}} \right) \quad (64)$$

The proof is similar to the proof of formula (51) which can be found in Appendix.

4.5. Heuristic Algorithms, based on KKT-analysis

Algorithm 1: Heuristic Intersection Method of Power Allocation using Conjugate Detection and effective $SINR$ as the geometrical mean

Input: Channel \mathbf{H} and its decomposition $\mathbf{H} = \mathbf{U}^H \mathbf{S} \mathbf{V}$ by Lemma 2.1, precoding matrix $\mathbf{W}(\mathbf{V})$, station power P , number of base station antennas T and noise σ^2 ;

Calculate starting point $\mathbf{P}_1 : (\mathbf{p}_1)_l = \frac{P/T}{\|\mathbf{w}_l\|^2}$

Calculate the hyperplane on which the square of starting point lies. Index of this hyperplane $i(\mathbf{P}_1) = \arg \max(\text{row_norm}(\mathbf{W}\mathbf{P}_1))$;

Calculate optimal point on this hyperplane $\mathbf{P}_2 : (\mathbf{p}_2)_l = \frac{P}{TL\|\mathbf{w}_l\|^2}$

if \mathbf{P}_2 satisfies to Power Constraints **then**

 | **return** $\mathbf{W}_{opt} = \mathbf{W}\mathbf{P}_2$

else

 | **Calculate** direction vector $\mathbf{d} = \mathbf{P}_2^2 - \mathbf{P}_1^2$

 | **Calculate** first intersection \mathbf{P}_{opt}^2 on a beam $\{\mathbf{P}_1^2 + \alpha\mathbf{d} | \alpha > 0\}$ with other hyperlanes.

 | **return** $\mathbf{W}_{opt} = \mathbf{W}\mathbf{P}_{opt}$

end

We compare different power allocations applied to the different reference algorithms (ZF, RZF, ARZF). Primarily, the comparison involves precoding with base powers (native methods without PA) and the power equalization algorithm (46). Also, we consider some algorithms based on Karush–Kuhn–Tucker conditions (56).

The algorithms take equalizing powers as the first approximation of the vector \mathbf{p} (See Point 1 on Fig. 3). Then it finds the hyperplane on which the given point lies and searches on this hyperplane for the optimal (Point 2). To find the optimal point we use the formula (58) for the first algorithm and by formula (63) for the second algorithm. If the obtained point is satisfied with the Power Constraints then this is the result of the algorithm. This point may not be satisfied with the Power Constraints. In this case, we construct a beam from starting point to the optimal point. The first intersection with other hyperplanes (Point 3) is a result of the algorithms.

Remark 6. The formula for Point 2 can be negative or zero. This is a rare case. In this case, the result of the algorithm is Point 1.

5. Simulation Results

We describe the generation process in detail in our work [7]. To generate channel coefficients, we use Quadriga [18], open-source software for generating realistic radio channel impulse responses. We consider the Urban Quadriga scenario. For each seed, we generate the random sets of user positions (see example in Fig 4) and compute channel matrices for the obtained user configurations.

In Fig. 2, we present numerical simulations of the proposed Intersection Method (1)

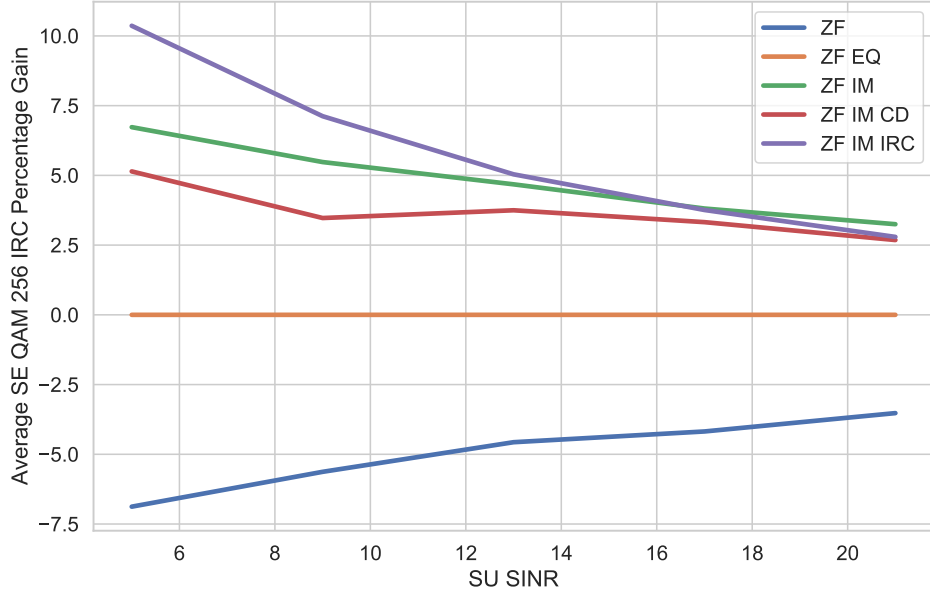
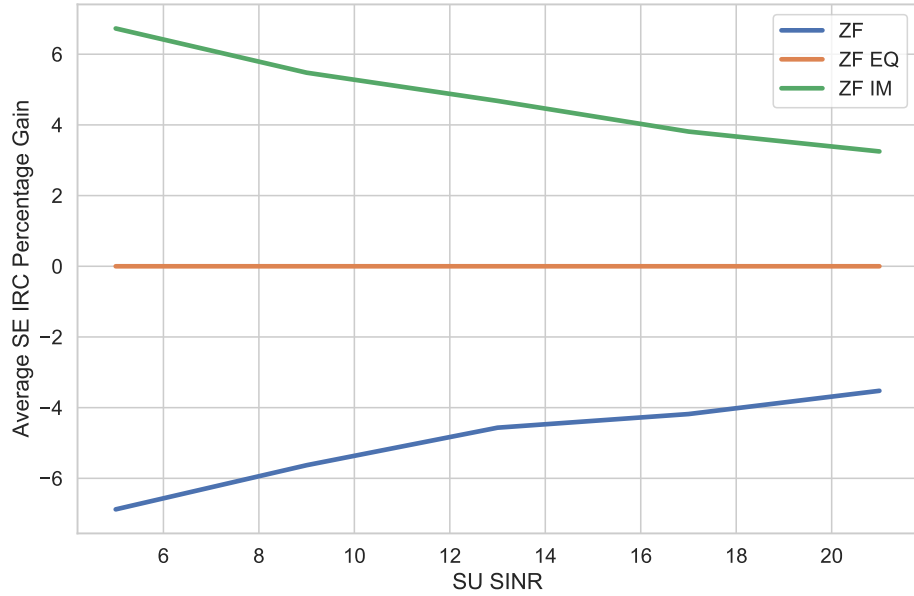


Figure 2. Average SE gains assuming Geometric Mean Effective SINR (37) (Upper) and QAM256 (15) (Lower) of the different Power Allocation algorithms.

Algorithm 2: Heuristic Intersection Method of Power Allocation using MMSE
IRC Detection and effective $SINR$ as QAM64 or QAM256

Input: Channel \mathbf{H} and its decomposition $\mathbf{H} = \mathbf{U}^H \mathbf{S} \mathbf{V}$ by Lemma 2.1, station power P , noise σ^2 ;

Define smooth precoding function $\mathbf{W}(\mathbf{V})$;

Define smooth detection function $\mathbf{G}(\mathbf{H}, \mathbf{W})$ using MMSE-IRC (11) or CD (13);

Define smooth target function $J(\mathbf{P})$. For example $J^{SE}(\mathbf{P}) = SE(\mathbf{W}' \mathbf{P}, \mathbf{H}, \mathbf{G}, \sigma^2)$ using (14), (16) and (15);

Calculate starting point $\mathbf{P}_1 : (\mathbf{p}_1)_l = \frac{P/T}{\|\mathbf{w}_l\|^2}$ (58)

Calculate the hyperplane on which the square of starting point lies. Index of this hyperplane $i(\mathbf{P}_1) = \arg \max(\text{row_norm}(\mathbf{W} \mathbf{P}_1))$;

Calculate the optimal point on this hyperplane $\mathbf{P}_2 = \arg \max(J^{SE}(\mathbf{P}))$ (63)

if $\|\mathbf{P}_1\|_\infty < 0$ **then**

 | **return** $\mathbf{W}_{opt} = \mathbf{W} \mathbf{P}_1$

end

if \mathbf{P}_2 *satisfies to Power Constraints* **then**

 | **return** $\mathbf{W}_{opt} = \mathbf{W} \mathbf{P}_2$

else

 | **Calculate** direction vector $\mathbf{d} = \mathbf{P}_2^2 - \mathbf{P}_1^2$

 | **Calculate** first intersection \mathbf{P}_{opt}^2 on a beam $\{\mathbf{P}_1^2 + \alpha \mathbf{d} | \alpha > 0\}$ with other hyper-lines.

 | **return** $\mathbf{W}_{opt} = \mathbf{W} \mathbf{P}_{opt}^2$

end

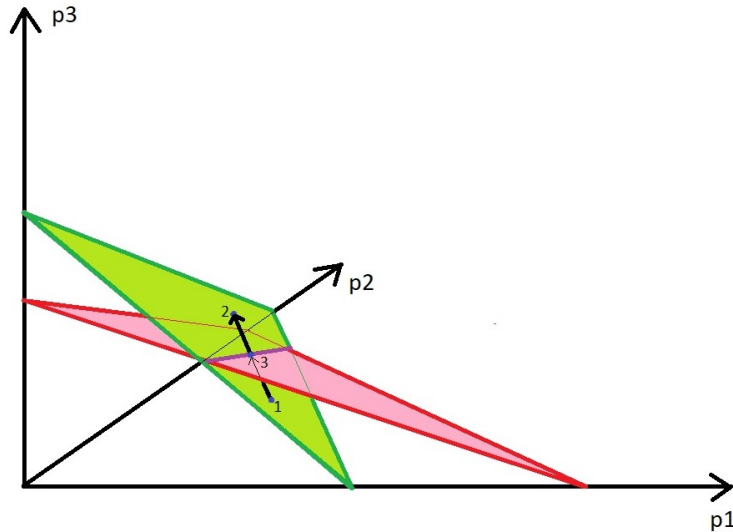


Figure 3. Geometrical illustration of the Intersection Method of Power Allocation 1 with a small layer space ($L = 3$). Point 1 is the first approximation for solution of the algorithm and lies on the green hyperplane. Point 2 is the optimal Point on the green hyperplane, which we obtain as a solution to the Lagrange problem (58). The red hyperplane contains the closest intersection of the beam from Point 1 to Point 2 concerning other hyperplanes. Point 3 is the intersection of the beam from Point 1 to Point 2 on the red hyperplane. If Point 3 lies between Points 1 and 2, it is a solution of the algorithms, otherwise, a solution is Point 2.

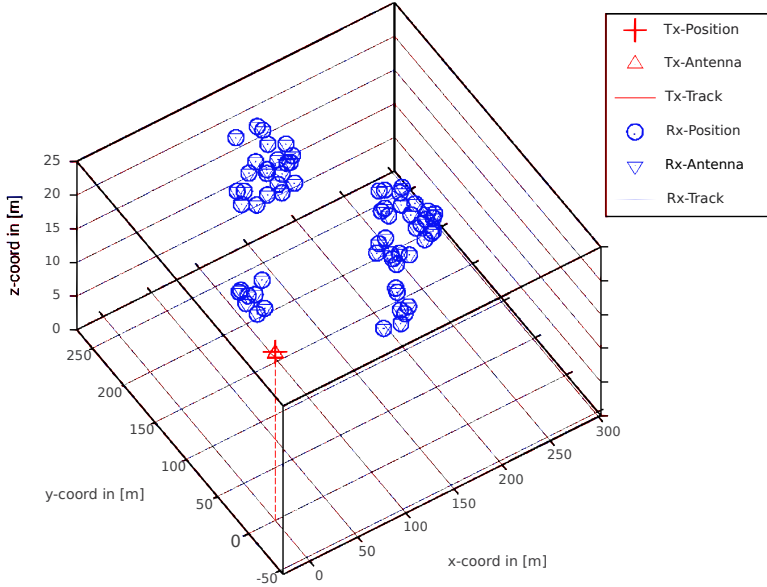


Figure 4. Example of the random generation of users for Urban setup. There are two buildings, and the users are assigned to either a cluster in a building or to the ground near the building [7] .

(ZF IM) with its modifications to QAM model (2) (ZF IM CD, ZF IM IRC) and reference Naive (ZF) and Equal Power (ZF EQ) methods. Both pictures show the average spectral efficiency gain over the Equal Power method. The left picture shows SE gain assuming Geometric Mean Effective SINR (37), while the right one assumes the QAM256 model (15). Both (ZF IM) and (ZF IM IRC) algorithms provide better power allocation (PA) under per-antenna power constraint (PAPC).

The experiments show that the proposed method (ZF IM) outperforms the reference (ZF EQ) up to 6% at the low *SUSINR* region (< 5 dB) and up to 3% at high (> 20 dB). The modification of the algorithm (ZF IM IRC) provides better results up to 10% at the low *SUSINR* region. It turned out that the modification (ZF IM CD) provides worse results than (ZF IM). This can be explained by the fact that final quality is measured using MMSE-IRC 11 detection matrix.

6. Conclusion

In this work, we studied the power allocation (PA) problem of wireless MIMO systems with multi-antenna users. We presented solutions to the PA problem, which maximize the network throughput in terms of spectral efficiency (SE). Since the initial problem is non-convex, it was equivalently reformulated as a Lagrange problem by simplifying the MMSE-IRC detection and the SE function. We obtained (i) an equal power exact solution of PA under total power constraint (TPC) and (ii) an algorithmic solution of PA for per-antenna power constraints (PAPC) based on a system of Lagrange equations and geometric view of the problem. Simulation results show the effectiveness of the proposed algorithmic approach over the reference PA schemes. The proposed PA method makes it possible to improve the quality of MIMO systems in the future.

References

- [1] A.C. Aitken, *IV.—On least squares and linear combination of observations*, Proceedings of the Royal Society of Edinburgh 55 (1936), pp. 42–48.
- [2] J.G. Andrews, S. Buzzi, W. Choi, S.V. Hanly, A. Lozano, A.C. Soong, and J.C. Zhang, *What will 5G be?*, IEEE Journal on selected areas in communications 32 (2014), pp. 1065–1082.
- [3] E. Björnson, M. Bengtsson, and B. Ottersten, *Optimal multiuser transmit beamforming: A difficult problem with a simple solution structure [lecture notes]*, IEEE Signal Processing Magazine 31 (2014), pp. 142–148.
- [4] E. Björnson, J. Hoydis, and L. Sanguinetti, *Massive MIMO networks: Spectral, energy, and hardware efficiency*, Foundations and Trends in Signal Processing 11 (2017), pp. 154–655.
- [5] E. Björnson and E. Jorswieck, *Optimal resource allocation in coordinated multi-cell systems*, Now Publishers Inc, 2013.
- [6] E. Björnson, E. Jorswieck, and B. Ottersten, *Impact of spatial correlation and precoding design in OSTBC MIMO systems*, IEEE Transactions on Wireless Communications 9 (2010), pp. 3578–3589.
- [7] E. Bobrov, B. Chinyaev, V. Kuznetsov, H. Lu, D. Minenkov, S. Troshin, D. Yudakov, and D. Zaev, *Adaptive regularized zero-forcing beamforming in Massive MIMO with multi-antenna users*, arXiv preprint arXiv:2107.00853 (2021).
- [8] E. Bobrov, D. Kropotov, and H. Lu, *Massive MIMO adaptive modulation and coding using online deep learning algorithm*, IEEE Communications Letters (2021).
- [9] E. Bobrov, D. Kropotov, S. Troshin, and D. Zaev, *L-BFGS precoding optimization algorithm for massive MIMO systems with multi-antenna users* (2021).
- [10] E. Bobrov, A. Markov, and D. Vetrov, *Variational autoencoders for studying the manifold of precoding matrices with high spectral efficiency*, arXiv preprint arXiv:2111.15626 (2021).
- [11] F. Boccardi and H. Huang, *Optimum power allocation for the MIMO-BC zero-forcing precoder with per-antenna power constraints*, in *2006 40th Annual Conference on Information Sciences and Systems*. IEEE, 2006, pp. 504–504.
- [12] X. Deng and A.M. Haimovich, *Power allocation for cooperative relaying in wireless networks*, IEEE Communications Letters 9 (2005), pp. 994–996.
- [13] S. Dhakal, *High rate signal processing schemes for correlated channels in 5G networks*. (2019).
- [14] N. Fatema, G. Hua, Y. Xiang, D. Peng, and I. Natgunanathan, *Massive MIMO linear precoding: A survey*, IEEE systems journal 12 (2017), pp. 3920–3931.
- [15] X. Ge, R. Zi, H. Wang, J. Zhang, and M. Jo, *Multi-user massive MIMO communication systems based on irregular antenna arrays*, IEEE Transactions on Wireless Communications 15 (2016), pp. 5287–5301.
- [16] Z. Hanzaz and H.D. Schotten, *Analysis of effective SINR mapping models for MIMO OFDM in LTE system* (2013), pp. 1509–1515.
- [17] A. Host-Madsen and J. Zhang, *Capacity bounds and power allocation for wireless relay channels*, IEEE transactions on Information Theory 51 (2005), pp. 2020–2040.
- [18] S. Jaeckel, L. Raschkowski, K. Börner, and L. Thiele, *QuaDRiGa: A 3-D multi-cell channel model with time evolution for enabling virtual field trials*, IEEE Transactions on Antennas and Propagation 62 (2014), pp. 3242–3256.
- [19] M. Joham, W. Utschick, and J.A. Nossek, *Linear transmit processing in MIMO communications systems*, IEEE Transactions on signal Processing 53 (2005), pp. 2700–2712.
- [20] S. Lagen, K. Wanuga, H. Elkotby, S. Goyal, N. Patriciello, and L. Giupponi, *New radio physical layer abstraction for system-level simulations of 5G networks*, in *ICC 2020-2020 IEEE International Conference on Communications (ICC)*. IEEE, 2020, pp. 1–7.
- [21] L. Le and E. Hossain, *Multihop cellular networks: Potential gains, research challenges, and a resource allocation framework*, IEEE Communications Magazine 45 (2007), pp. 66–73.

- [22] Y. Liang and V.V. Veeravalli, *Gaussian orthogonal relay channels: Optimal resource allocation and capacity*, IEEE Transactions on Information Theory 51 (2005), pp. 3284–3289.
- [23] N.H. Mahmood, G. Berardinelli, F.M. Tavares, M. Lauridsen, P. Mogensen, and K. Pa-jukoski, *An efficient rank adaptation algorithm for cellular MIMO systems with IRC receivers*, in *2014 IEEE 79th Vehicular Technology Conference (VTC Spring)*. IEEE, 2014, pp. 1–5.
- [24] T.L. Marzetta, *Noncooperative cellular wireless with unlimited numbers of base station antennas*, IEEE transactions on wireless communications 9 (2010), pp. 3590–3600.
- [25] A.H. Mehana and A. Nosratinia, *Diversity of MMSE MIMO receivers*, IEEE Transactions on information theory 58 (2012), pp. 6788–6805.
- [26] H.Q. Ngo, E.G. Larsson, and T.L. Marzetta, *Energy and spectral efficiency of very large multiuser MIMO systems*, IEEE Transactions on Communications 61 (2013), pp. 1436–1449.
- [27] D.H. Nguyen and H.H. Nguyen, *Power allocation in wireless multiuser multi-relay networks with distributed beamforming*, IET communications 5 (2011), pp. 2040–2051.
- [28] T. Parfait, Y. Kuang, and K. Jerry, *Performance analysis and comparison of ZF and MRT based downlink massive MIMO systems*, in *2014 sixth international conference on ubiquitous and future networks (ICUFN)*. IEEE, 2014, pp. 383–388.
- [29] K.T. Phan, T. Le-Ngoc, S.A. Vorobyov, and C. Tellambura, *Power allocation in wireless multi-user relay networks*, IEEE Transactions on Wireless Communications 8 (2009), pp. 2535–2545.
- [30] B. Ren, Y. Wang, S. Sun, Y. Zhang, X. Dai, and K. Niu, *Low-complexity MMSE-IRC algorithm for uplink massive MIMO systems*, Electronics Letters 53 (2017), pp. 972–974.
- [31] L. Sanguinetti, A. Zappone, and M. Debbah, *Deep learning power allocation in massive MIMO*, in *2018 52nd Asilomar conference on signals, systems, and computers*. IEEE, 2018, pp. 1257–1261.
- [32] S. Shi, M. Schubert, and H. Boche, *Downlink MMSE transceiver optimization for multiuser MIMO systems: Duality and sum-MSE minimization*, IEEE Transactions on Signal Processing 55 (2007), pp. 5436–5446.
- [33] L. Sun and M.R. McKay, *Eigen-based transceivers for the MIMO broadcast channel with semi-orthogonal user selection*, IEEE Transactions on Signal Processing 58 (2010), pp. 5246–5261.
- [34] D. Tse and P. Viswanath, *Fundamentals of wireless communication*, Cambridge university press, 2005.
- [35] T. Van Chien, E. Björnson, and E.G. Larsson, *Joint power allocation and load balancing optimization for energy-efficient cell-free massive MIMO networks*, IEEE Transactions on Wireless Communications 19 (2020), pp. 6798–6812.
- [36] S. Verdú, *Spectral efficiency in the wideband regime*, IEEE Transactions on Information Theory 48 (2002), pp. 1319–1343.
- [37] B. Wang, Y. Chang, and D. Yang, *On the SINR in massive MIMO networks with MMSE receivers*, IEEE Communications Letters 18 (2014), pp. 1979–1982.
- [38] Z. Wang and W. Chen, *Regularized zero-forcing for multiantenna broadcast channels with user selection*, IEEE Wireless Communications Letters 1 (2012), pp. 129–132.
- [39] D. Wubben, R. Bohnke, V. Kuhn, and K.D. Kammeyer, *Near-maximum-likelihood detection of MIMO systems using MMSE-based lattice-reduction*, in *2004 IEEE International Conference on Communications (IEEE Cat. No. 04CH37577)*, Vol. 2. IEEE, 2004, pp. 798–802.
- [40] T. Yoo and A. Goldsmith, *On the optimality of multiantenna broadcast scheduling using zero-forcing beamforming*, IEEE Journal on selected areas in communications 24 (2006), pp. 528–541.
- [41] W. Yu, *Uplink-downlink duality via minimax duality*, IEEE Transactions on Information Theory 52 (2006), pp. 361–374.
- [42] A. Zaidi, F. Athley, J. Medbo, U. Gustavsson, G. Durisi, and X. Chen, *5G Physical Layer: principles, models and technology components*, Academic Press, 2018.

- [43] J. Zhang, S. Chen, R.G. Maunder, R. Zhang, and L. Hanzo, *Regularized zero-forcing precoding-aided adaptive coding and modulation for large-scale antenna array-based air-to-air communications*, IEEE Journal on Selected Areas in Communications 36 (2018), pp. 2087–2103.
- [44] Y. Zhao, R. Adve, and T.J. Lim, *Improving amplify-and-forward relay networks: optimal power allocation versus selection*, in *2006 ieee international symposium on information theory*. IEEE, 2006, pp. 1234–1238.
- [45] K. Zheng, L. Zhao, J. Mei, B. Shao, W. Xiang, and L. Hanzo, *Survey of large-scale MIMO systems*, IEEE Communications Surveys & Tutorials 17 (2015), pp. 1738–1760.

Appendix

6.1. MCS – beta – SINR eff

The values of β for Modulation and Coding Schemes (MCS) [8] are taken from Table 2. There are different β values for different QAMs [20]. The Table 2 shows the most popular cases: QAM 64 and QAM 256. The MCS value depends on the radio quality and therefore on $SINR_{eff}$. For the MCS value, a fairly accurate estimate is

$$MCS \approx SINR_{eff}(dB) + 5 \quad (65)$$

Thus, $SINR_{eff}$ can be found by solving a system of two equations, (15) and (65), taking $\beta = \beta(MCS)$. Also note that low values of $SINR_{eff}$ (up to -5dB) indicate that the user is almost out of service, and high values of $SINR_{eff}$ (after 23dB) do not make much sense.

6.2. Formulas

Proof of formula (51):

From $\mathcal{L}'_{p_l} = 0$:

$$x_l = (1 - \beta_k \ln(X_k)) X_k \beta_k \sigma^2 \|\mathbf{g}_l\|^2 \lambda_1 \|\mathbf{w}'_l\|^2 \quad (66)$$

$$X_k = \frac{1}{L_k} \sum_{l=1}^{L_k} x_l = (1 - \beta_k \ln(X_k)) X_k \frac{1}{L_k} \sum_{l=1}^{L_k} (\beta_k \sigma^2 \|\mathbf{g}_l\|^2 \lambda_1 \|\mathbf{w}'_l\|^2) \quad (67)$$

$$\frac{x_l}{X_k} = \frac{\beta_k \sigma^2 \|\mathbf{g}_l\|^2 \lambda_1 \|\mathbf{w}'_l\|^2}{\frac{1}{L_k} \sum_{s=1}^{L_k} (\beta_k \sigma^2 \|\mathbf{g}_s\|^2 \lambda_1 \|\mathbf{w}'_s\|^2)} = \frac{\|\mathbf{g}_l\|^2 \|\mathbf{w}'_l\|^2}{\frac{1}{L_k} \sum_{s=1}^{L_k} (\|\mathbf{g}_s\|^2 \|\mathbf{w}'_s\|^2)} \quad (68)$$

From (67):

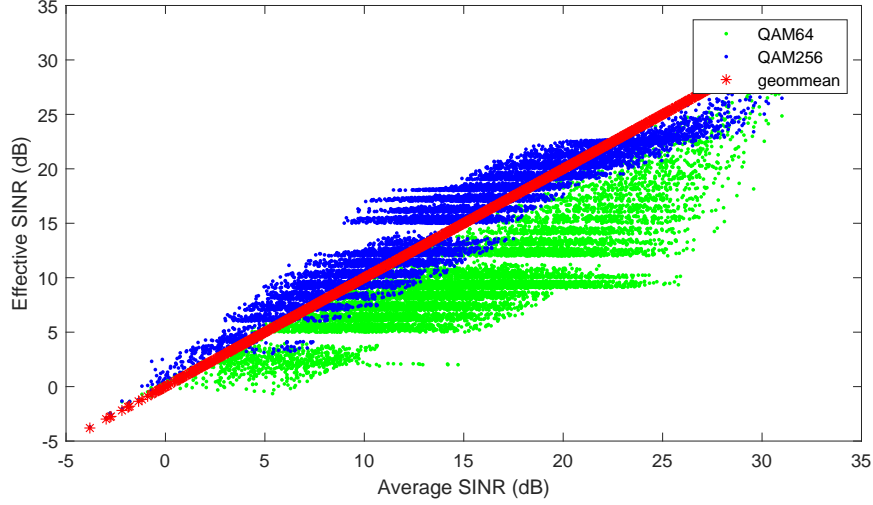


Figure 5. Approximation $SINR_{\text{eff}}$

$$X_k = \exp\left(\frac{1}{\beta_k}\right) \exp\left(1 - \frac{1}{\frac{1}{L_k} \sum_{l=1}^{L_k} (\beta_k \sigma^2 \|\mathbf{g}_l\|^2 \lambda_1 \|\mathbf{w}'_l\|^2)}\right) = f_k(\lambda_1) \quad (69)$$

Taking into account $\sum_{l=1}^L (\|\mathbf{w}'_l\|^2 p_l) = P$ we obtain:

$$\begin{aligned} \sum_{l=1}^L (\|\mathbf{w}'_l\|^2 p_l) &= - \sum_{l=1}^L \sigma^2 \|\mathbf{g}_l\|^2 \|\mathbf{w}'_l\|^2 \left(1 - \frac{1}{\frac{1}{L_k} \sum_{s=1}^{L_k} (\beta_k \sigma^2 \|\mathbf{g}_s\|^2 \lambda_1 \|\mathbf{w}'_s\|^2)} \right) - \\ &\quad - \sum_{l=1}^L \beta_k \sigma^2 \|\mathbf{g}_l\|^2 \|\mathbf{w}'_l\|^2 \ln \left(\frac{\|\mathbf{g}_l\|^2 \|\mathbf{w}'_l\|^2}{\frac{1}{L_k} \sum_{s=1}^{L_k} \|\mathbf{g}_s\|^2 \|\mathbf{w}'_s\|^2} \right) = P \quad (70) \end{aligned}$$

$$\lambda_1^{-1} = \frac{P + \sum_{l=1}^L \beta_k \sigma^2 \|\mathbf{g}_l\|^2 \|\mathbf{w}'_l\|^2 \ln \left(\frac{\|\mathbf{g}_l\|^2 \|\mathbf{w}'_l\|^2}{\frac{1}{L_k} \sum_{s=1}^{L_k} \|\mathbf{g}_s\|^2 \|\mathbf{w}'_s\|^2} \right) + \sum_{l=1}^L \sigma^2 \|\mathbf{g}_l\|^2 \|\mathbf{w}'_l\|^2}{\sum_{l=1}^L \frac{\sigma^2 \|\mathbf{g}_l\|^2 \|\mathbf{w}'_l\|^2}{\frac{1}{L_k} \sum_{s=1}^{L_k} (\beta_k \sigma^2 \|\mathbf{g}_s\|^2 \|\mathbf{w}'_s\|^2)}} \quad (71)$$

Substituting (71) into (69) and (69) into (66) we get expressions for x_l and hence for p_l .

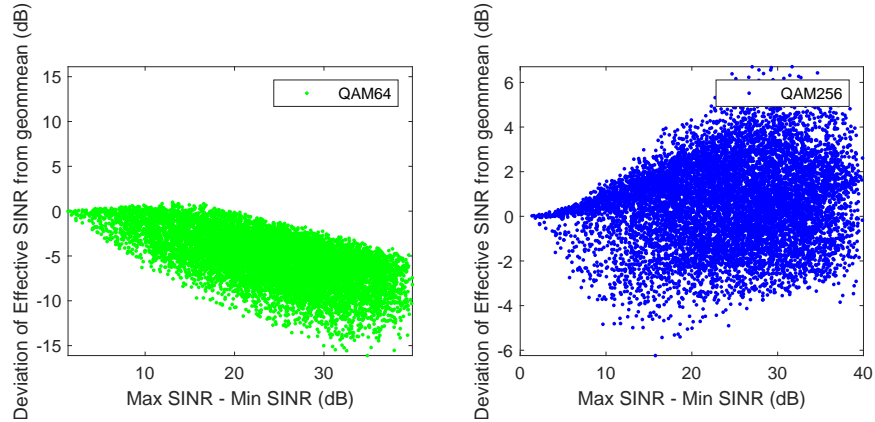


Figure 6. Deviation of $SINR_{\text{eff}}$

MCS	QAM 64	QAM 256	MCS	QAM 64	QAM 256
0	1.6	1.6	15	6.16	19.33
1	1.61	1.63	16	6.5	21.85
2	1.63	1.67	17	9.95	24.51
3	1.65	1.73	18	10.97	27.14
4	1.67	1.79	19	12.92	29.94
5	1.7	4.27	20	14.96	56.48
6	1.73	4.71	21	17.06	65
7	1.76	5.16	22	19.33	78.58
8	1.79	5.66	23	21.85	92.48
9	1.82	6.16	24	24.51	106.27
10	3.97	6.5	25	27.14	118.74
11	4.27	10.97	26	29.94	126.36
12	4.71	12.92	27	32.05	132.54
13	5.16	14.96	28	34.28	
14	5.66	17.06			

Table 2. Table of QAM 64 and QAM 256 beta values [20] .